metals

MDPI

Article

FeSiCr-Based Soft Magnetic Composites with SiO_2 Insulation Coating Prepared Using the Elemental Silicon Powder Hydrolysis Method

Chunlong Li [1], Hongya Yu [2,3,*], Guangze Han [1,3,*] and Zhongwu Liu [2]

[1] School of Physics and Optoelectronics, South China University of Technology, Guangzhou 510640, China
[2] School of Materials Science and Engineering, South China University of Technology, Guangzhou 510640, China
[3] Dongguan Mentech Optical & Magnetic Co., Ltd., Dongguan 523330, China
* Correspondence: yuhongya@scut.edu.cn (H.Y.); phgzhan@scut.edu.cn (G.H.)

Abstract: In this work, FeSiCr powders were coated with a SiO_2 insulation layer for soft magnetic composites (SMCs) through elemental silicon powder hydrolysis, without using any expensive precursors. The effects of the reaction temperature and ammonia concentration on the structure and performance of SMCs were investigated. Through the elemental silicon powder hydrolysis process, the formation of an FeSiCr–SiO_2 core-shell structure effectively reduced the core loss, increased resistivity, and improved the quality factor of SMCs. SMCs prepared with 0.10 mL/g ammonia concentration at 50 °C exhibited the best combination of properties, with saturation magnetization M_s = 169.40 emu/g, effective permeability μ_e = 40.46, resistivity $\rho = 7.1 \times 10^6$ Ω·cm, quality factor Q = 57.07 at 1 MHz, and core loss P_s = 493.3 kW/m^3 at 50 mT/100 kHz. Compared to the uncoated sample, SMCs with a SiO_2 coating exhibit 23% reduction in P_s, with only 6.6% reduction in μ_e. Compared to SMCs fabricated using the traditional sol-gel method, the sample prepared through hydrolysis of elemental silicon powder has higher permeability and lower core loss. In particular, this new approach gives an effective coat solution for the mass production of high-temperature-resistant SMCs.

Keywords: soft magnetic composites; silica insulation coating; hydrolysis method; magnetic properties; core loss

check for updates

Citation: Li, C.; Yu, H.; Han, G.; Liu, Z. FeSiCr-Based Soft Magnetic Composites with SiO_2 Insulation Coating Prepared Using the Elemental Silicon Powder Hydrolysis Method. *Metals* **2023**, *13*, 1444. https://doi.org/10.3390/met13081444

Academic Editor: Evangelos Hristoforou

Received: 22 July 2023
Revised: 5 August 2023
Accepted: 8 August 2023
Published: 11 August 2023

1. Introduction

Soft magnetic composites (SMCs), also known as magnetic powder cores, are made of magnetic powders coated with a high-resistivity insulation layer, followed by a condensation process [1–4]. Having both the highly saturated magnetization ability of metallic materials and excellent insulation characteristics of non-metallic materials, SMCs are an attractive class of soft magnetic materials [5]. They are expected to be widely applied in devices and components used in electronic systems, such as inductors, transformers, motors, etc. [6,7]. At present, electronic devices are developing toward high-saturation magnetization, high effective permeability, high frequency, and low core loss [8–11], which requires higher temperature resistance, better corrosion resistance, and a stronger insulation of magnetic powder cores. Conventional magnetic powder cores include pure iron powder cores, hi-flux (Fe–Ni) powder cores, FeSiAl powder cores, iron silicon magnetic powder cores, amorphous nanocrystalline magnetic powder cores, etc. [12]. Among them, FeSiCr magnetic powder cores are prepared by adding Si and Cr elements to iron powder, as reported in recent years [13–15]. Introduction of the Si element can increase resistivity and reduce core loss. The addition of the Cr element can significantly improve the plasticity, corrosion resistance, and oxidation resistance. Hence, FeSiCr magnetic powder cores have strong aging resistance at high temperatures [16].

With the increase in application frequency, the temperature rises and core loss become significant in SMCs [17,18]. The introduction of an insulation coating on the powder surface has become necessary in order to increase the resistivity of the metallic powder [19]. As established, silica has excellent temperature resistance, high corrosion resistance and electric resistivity. It is a good material for insulation coating of magnetic powders. Furthermore, silica coating can enhance the stability and prevent the agglomeration of the powder in solvents, so it has been widely used in soft magnetic cores in recent years. Hsiang et al. [20] improved the resistivity and DC bias superposition of FeSiCr powder by coating with an amorphous silica layer on the powder using the water glass method. Wu et al. [21] fabricated iron-based soft magnetic composites coated with an amorphous SiO_2 layer through the reverse microemulsion method, significantly reducing the core loss of iron-based SMCs. Luo et al. [22] prepared Fe-6.5wt.%Si@SiO_2 SMCs using in situ chemical deposition followed by the spark plasma sintering (SPS) process, and investigated the effects of ammonia concentration on the microstructure and magnetic properties. Cheng et al. [23] prepared iron particles coated with silica using the sol-gel method, and improved the oxidation resistance of sample. However, these silica coating methods have some drawbacks such as being complex processes, requiring harsh reaction conditions, or having a high preparation cost, which is not preferred for large-scale production in industry. Recently, Lim et al. [24] prepared a silicon sol with controllable particle size and good mono-dispersity through elemental silicon hydrolysis. By adjusting the reaction temperature and amount of catalyst, the size of silica nanoparticles can be controlled [25,26]. Wang et al. [27] used the elemental silicon hydrolysis coating method for the first time to coat silica and achieve Fe_3O_4@SiO_2 colloidal dispersion. However, the hydrolysis of elemental silicon has not yet been used as an insulation coating for magnetic powder.

In this work, silica was coated on the surface of FeSiCr soft magnetic powders through the hydrolysis of silicon powder, using elemental silicon powder as the source and ammonia as the catalytic agent. The influences of the reaction temperature and ammonia concentration on magnetic properties of FeSiCr@SiO_2 SMCs have been systematically investigated. The results show that the SMCs insulated by silica nanoparticles have significantly improved resistivity, core loss, and quality factor. The proposed approach also has the advantages of being a simple process and having a low cost.

2. Experimental Protocol

The raw FeSiCr powder used in this work was prepared using the water atomization method, purchased from Antai Technology Co., Ltd. (Beijing, China). The powder has the composition of 87.9–89.3 wt.% Fe, 6.0–6.8 wt.% Si, and 4.7–5.3 wt.% Cr, and the average particle size is 10.3 μm. The elemental silicon powder with the particle size from 40 to 200 mesh (75–380 μm) was purchased from Shanghai Macklin Biochemical Technology Co., Ltd. (Shanghai, China), used as the silicon source for the hydrolysis reaction to obtain SiO_2 nanoparticles. PVP (polyvinyl pyrrolidone) was purchased from Shanghai Bio Science & Technology Co., Ltd. (Shanghai, China), and was used to improve the binding between the FeSiCr powder and SiO_2 nanoparticles. Ammonia hydroxide (NH_4OH, 25–28%) purchased from Guangzhou Chemical Reagent Factory (Guangzhou, China) was used as catalyst. Typically, 100 g of FeSiCr powder is added to the anhydrous ethanol solution, with 2 g of PVP (polyvinyl pyrrolidone) dispersed. After stirring at room temperature for 20 min, the filtration separation is carried out to obtain the surface-modified FeSiCr powder. A certain concentration of ammonia hydroxide (NH_4OH, 25–28%) is added via pouring and ultrasonic-dispersed in 150 mL of deionized water. Then, 4 g elemental silicon powder is added into the ammonia solution. The mixture is stirred at a certain temperature for 3 h, and then the reaction solution passed through 800-mesh (18 μm) screens to remove excess silicon powder and obtain silica nanoparticle dispersion. The surface-modified FeSiCr powder was added into the silica nanoparticle dispersion, stirring at a certain temperature for 3 h. After removing the solvent through filtration, the residue was dried at 120 °C for 40 min and then the FeSiCr magnetic powder coated with silica was

obtained. The silica-coated powder was dipped into 2 wt.% silicon resin and 1 wt.% epoxy resin acetone solvent and stirred at room temperature until the acetone solvent evaporated completely. The resin-coated powder was pressed at 1200 MPa into magnetic ring SMCs with the dimensions of Φ20 × Φ12 × Φ4.8 mm, and then gradient heating at 180 °C for 20 min to cure the resin and obtain the final SMCs. For annealing treatment, the SMCs were heated at 500 °C for 1 h under Ar atmosphere.

The SiO_2-coating layers were characterized using Fourier transform infrared spectroscopy (FTIR, VERTEX 70, Billerica, MA, USA) to investigate the chemical structure. The surface morphologies and the element distribution of the powder were observed using a scanning electron microscope (SEM, FEI Quanta 200, Hillsboro, OR, USA) with energy-dispersive X-ray spectroscopy (EDS, EDAX Genesis Xm 2, Pleasanton, CA, USA). The hysteresis curves of the powders were measured at room temperature using a Vibrating Sample Magnetometer (VSM-3105, East Changing, Beijing, China). The electrical resistivity was measured using a high resistance weak current tester (ST2643, Jingge, Suzhou, China), with the voltage mode being used for testing, set to 50 V, and the data were recorded 1 min after starting the test. The core loss, loss angle tangent, and coercive force were tested with a soft magnetic AC measuring device (MATS-2010SA, Linkjoin, Loudi, China). An impedance analyzer (Agilent E4990A, Agilent, Kobe, Hyogo, Japan) was used to measure the permeability μ_e and quality factor Q of SMCs.

The hydrolytic coating of elemental silicon powder consists of two steps. In the first step, the surface of FeSiCr powder was pretreated with PVP. PVP was adsorbed on the surface of the FeSiCr powder for activation, acting as a bridge between the FeSiCr powder and SiO_2 nanoparticles. PVP molecule contains amide groups, which are positively charged in solution. In the second step, elemental silicon powder reacted with water under the catalysis of ammonia to generate silica nanoparticles with monodisperse and uniform size distribution in the solution. Then, the FeSiCr powder was added to the solution with SiO_2 nanoparticles, which have hydroxyl groups on the surface that are negatively charged in solution. Through the electrostatic adsorption and chemical reaction between the hydroxyl groups of SiO_2 nanoparticles and amide groups of PVP molecules, the SiO_2 nanoparticles can be coated on the surface of the FeSiCr magnetic powder. The reaction temperature will influence the rate of hydrolysis reaction and the generated amount of silica nanoparticles, while the ammonia concentration will affect the rate of reaction and the size of silica nanoparticles [25,26], so the experiment analyzes the effect of these parameters. The schematic diagram of the coating process is shown in Figure 1.

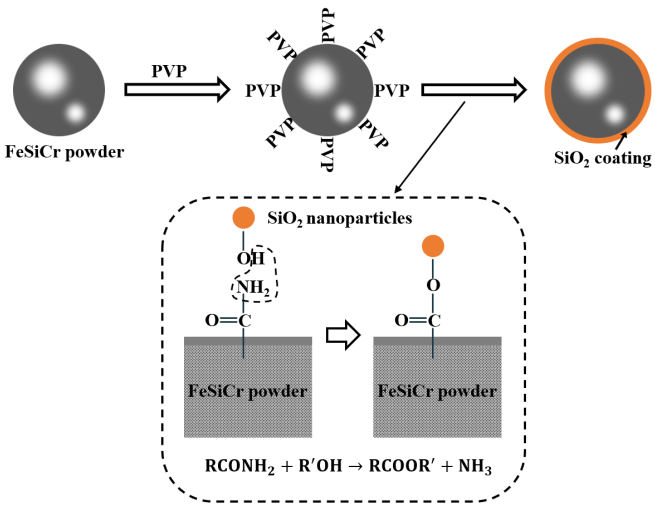

Figure 1. Schematic diagram for coating SiO_2 on an FeSiCr powder through the hydrolysis of elemental silicon powder.

Preparing the silica nanoparticles through the hydrolysis of elemental silicon powder is based on the following reaction equations:

$$Si + 2OH^- + H_2O \rightarrow SiO_3^{2-} + 2H_2 \quad (1)$$

$$SiO_3^{2-} + H_2O \rightarrow SiO_2 + 2OH^- \quad (2)$$

Ammonia plays a catalytic role, and the total reaction equation is:

$$Si + 2H_2O \xrightarrow{NH_4OH} SiO_2 + 2H_2 \quad (3)$$

3. Results and Discussion

3.1. Structure Analysis

Figure 2 shows the surface morphology of the FeSiCr raw powder and FeSiCr@SiO_2 powder prepared at different reaction temperatures. The surface of the raw powder is relatively smooth. For the sample prepared at 25 °C, particle aggregation can be found on the powder surface. Because there is no pre-activation process, the reaction proceeds very slowly so the coating effect is incomplete [25]. For the sample prepared at 40 °C, the area and quantity of particle aggregation increased compared to the sample prepared at 25 °C. For the sample prepared at 50 °C, the coating layer is more complete and some aggregation can be found. For the samples prepared at 60 °C and 70 °C, aggregation of the coating layer on the powder surface is more pronounced, and the uniformity of the coating layer is reduced. The reason is that as the temperature increases, the hydrolysis reaction is more rapid. The number and size of SiO_2 nanoparticles increase, and SiO_2 nanoparticles grow with heterogeneous nucleation [25].

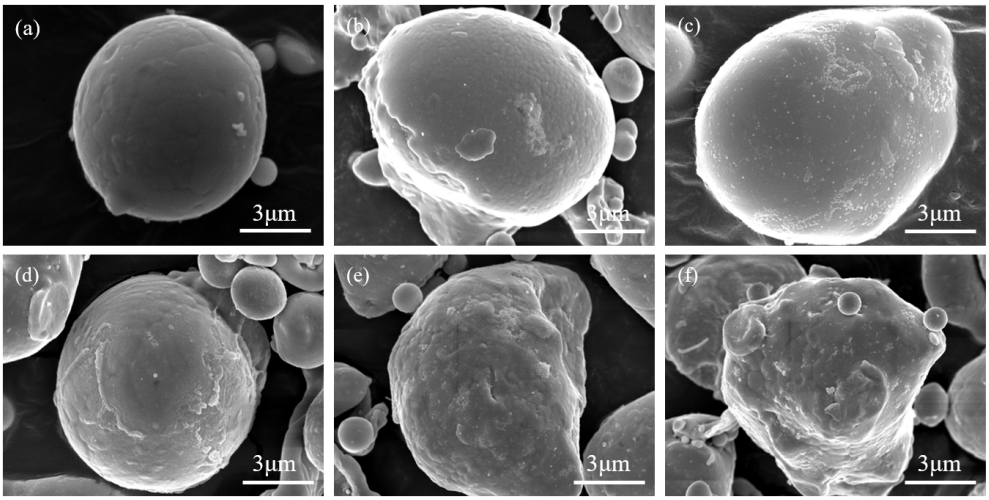

Figure 2. SEM micrograph of (**a**) the FeSiCr raw powder and the FeSiCr powder prepared through the hydrolysis of elemental silicon powder at different reaction temperatures: (**b**) 25 °C, (**c**) 40 °C, (**d**) 50 °C, (**e**) 60 °C, (**f**) 70 °C.

Figure 3a,b shows the SEM micrograph and EDS (energy-dispersive spectroscopy) elemental distributions of the FeSiCr raw powder and FeSiCr@SiO_2 powder prepared at 50 °C, respectively. The main elements of the FeSiCr raw powder are Fe, Si, and Cr. After SiO_2 coating at 50 °C, the O element appears on the surface of the powder, indicating that the SiO_2 layer has been successfully coated through the hydrolysis of elemental silicon powder. The O elements are evenly and completely distributed on the powder surface, indicating that the generated coating layer is complete and uniform, which is important for the insulation of the coating layer.

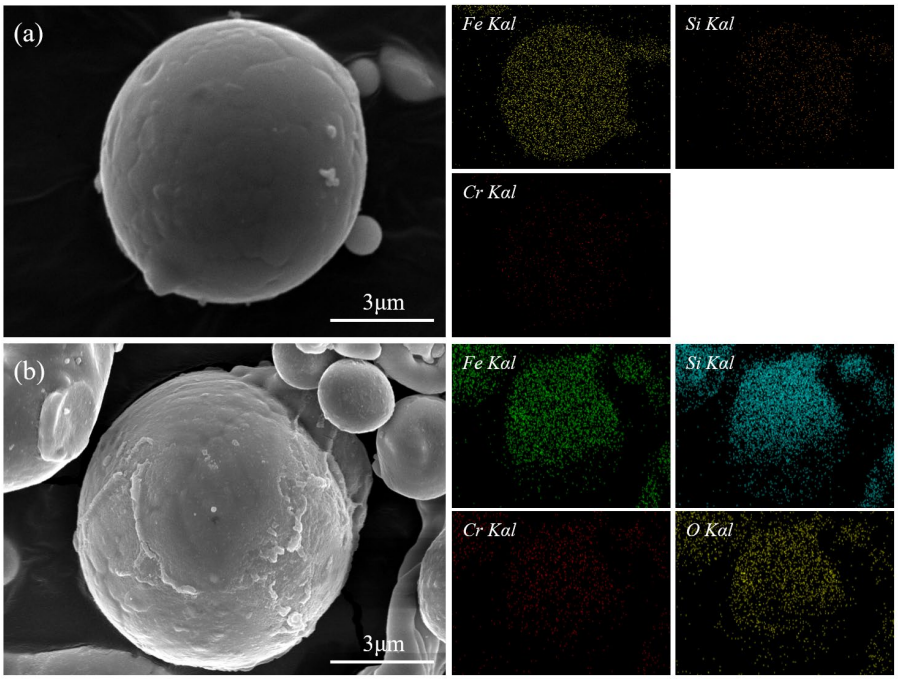

Figure 3. SEM micrograph and EDS analysis of (**a**) the FeSiCr raw powder, (**b**) FeSiCr powder prepared at 50 °C.

To further determine the structure and composition of the coating layer, the cross-section morphology, Fe, Si, Cr, and O elemental distributions through the mapping and line-scanning of SMCs are shown in Figure 4. The cross-section mapping scan shows that the Fe elements (Figure 4b) and Cr elements (Figure 4d) are mainly distributed in the matrix part of the magnetic powder, while the O elements (Figure 4e) are concentrated around the powder particles, which indicates that the coating layer on the surface of the FeSiCr magnetic powder is SiO_2. The line-scanning along the yellow line (Figure 4f) crossing the powder interface indicates that the Si and O elements increase, and the Fe and Cr elements decrease at the interface of the particles. This further indicates that the material of the coating layer is SiO_2. This coating effect is beneficial to improve insulation between the magnetic powders.

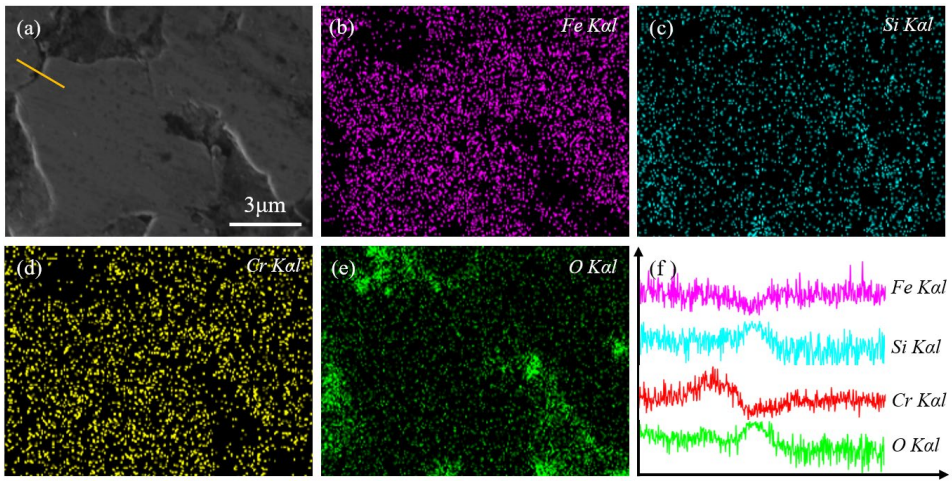

Figure 4. SEM micrograph and EDS analysis of the cross-section of FeSiCr@SiO_2 SMCs prepared at 50 °C: (**a**) SEM micrograph, (**b**–**f**) EDS mapping analysis of Fe, Si, Cr and O elemental, (**f**) EDS line-scanning of Fe, Si, Cr and O elemental.

Figure 5 shows the FTIR spectra of the FeSiCr raw powder and FeSiCr@SiO_2 powder prepared at 50 °C. The broad absorption bands around 3430 cm^{-1} and 1630 cm^{-1} are attributed to the stretching of -OH. The absorption band at 1068 cm^{-1} corresponds to the asymmetric vibration peak of the Si–O bond [28], and 466 cm^{-1} is the bending vibration peak of the Si–O bond [22,29]. After the coating of the powder, the intensity of the characteristic absorption peak of the Si–O bond is enhanced, further indicating that the coating layer is SiO_2.

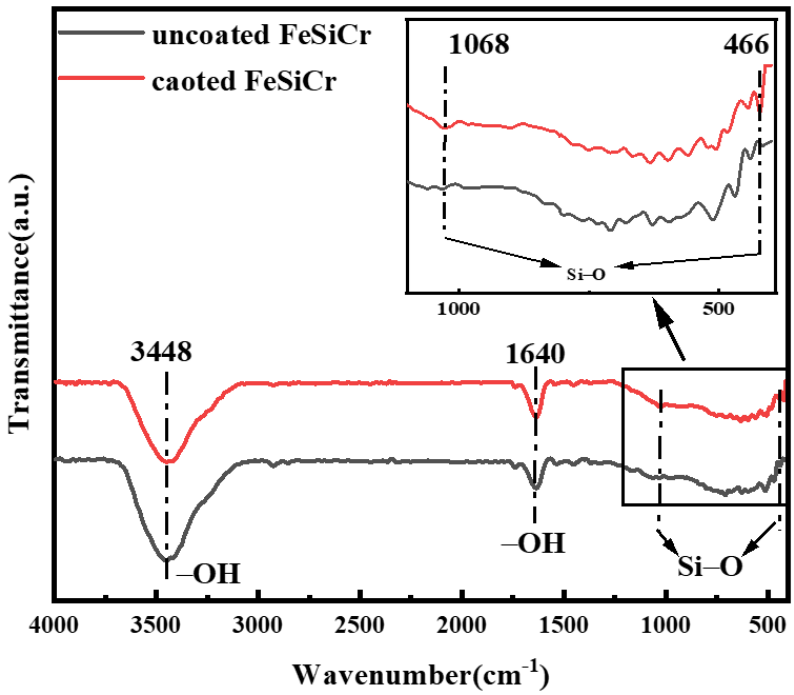

Figure 5. FTIR spectra of the FeSiCr powder before and after SiO_2 insulating through the hydrolysis of elemental silicon powder.

3.2. Effects of Reaction Temperature on Magnetic Properties

The reaction temperature was first optimized for the process and ammonia concentration is set to 0.10 mL/g. Figure 6 and Table 1 show the magnetic properties of SMCs prepared using the FeSiCr raw powder and FeSiCr@SiO_2 powder prepared with reaction temperatures of 25 °C, 40 °C, 50 °C, 60 °C, and 70 °C. The effective permeability μ_e in the frequency range from 20 kHz to 5 MHz is shown in Figure 6a. μ_e can be defined as follows:

$$\mu_e = \frac{L}{2hN^2\ln(D/d) \times 10^{-10}} \tag{4}$$

where L is the effective self-inductance, h is the height of the sample, N is the number of cooper wire turns, and D and d are the outer and inner diameters of the samples, respectively. The μ_e of the FeSiCr SMCs before and after SiO_2 coating have good frequency stability. Compared with the sample before coating, the introduction of non-magnetic-phase SiO_2 in the coated sample results in a magnetic dilution effect, which decreases the μ_e from 40.73 to 33.66. Compared to the samples prepared at 25 °C, 40 °C, and 50 °C, the μ_e of the samples prepared at 60 °C and 70 °C decrease more significantly. The reason is that the reaction temperature has an important effect on the growth of silica nanoparticles. When the temperature reaches above 60 °C, the reaction is more intense, and more silica nanoparticles are produced with larger particle size [25]. This leads to a more significant magnetic dilution effect. This can also be demonstrated by the resistivity of the samples, as shown in Figure 6d. When the reaction temperature reaches above 60 °C, there is

a significant increase in resistivity of the samples, which also indicates a significant increase in silica content.

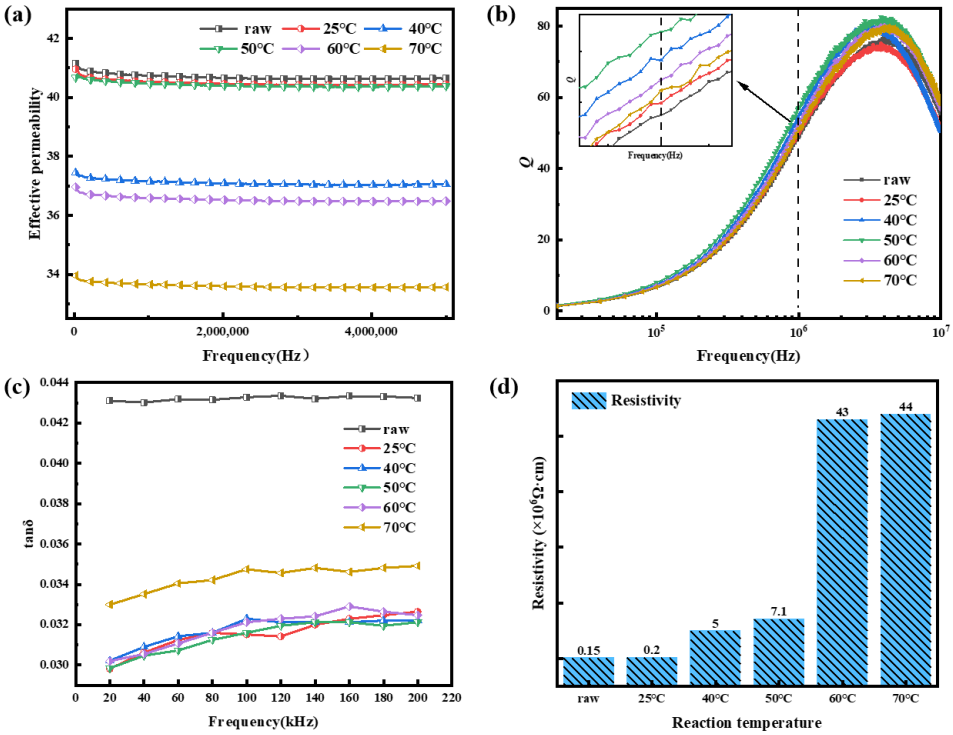

Figure 6. Magnetic properties of SMCs coated by elemental silicon powder through hydrolysis at different reaction temperatures: (**a**) effective permeability, (**b**) quality factor, (**c**) loss angle tangent, (**d**) resistivity.

Table 1. Magnetic properties of SMCs coated by elemental silicon powder through hydrolysis at different reaction temperatures.

Sample	ρ (Ω·cm)	μ_e (1 MHz)	Q (1 MHz)	P_s (kW/m^3) @ 50 mT	
				100 kHz	200 kHz
raw	1.5×10^5	40.73	46.70	707.4	1457
25 °C	2.0×10^5	40.63	49.89	587.1	1183
40 °C	5.0×10^6	40.59	54.09	509.4	1027
50 °C	7.1×10^6	40.46	57.06	493.3	987
60 °C	4.3×10^7	36.59	52.15	522.1	1052
70 °C	4.4×10^7	33.66	51.11	571.1	1154

The quality factor (Q) is a vital parameter for the electric component in the circuit. In general, the higher the Q value of the powder cores, the lower the rate of energy loss. The Q of the samples in the frequency range from 20 kHz to 10 MHz is shown in Figure 6b. All the samples show the same Q tendency of first rising then descending with the increasing frequency. At 1 MHz, the sample prepared with the FeSiCr raw powder has a low quality factor of 46.70, but the sample prepared at 50 °C has the highest quality factor of 57.07 due to the reduced core loss.

Figure 6c shows the loss angle tangent of the sample in the frequency range from 20 kHz to 5 MHz. The loss angle tangent is defined as the ratio between the imaginary part of permeability (μ'') and real part of permeability (μ'), which can be expressed by Equation (5):

$$\tan\delta = \frac{\mu''}{\mu'} \tag{5}$$

In Figure 6c, the loss angle tangent of SiO_2-coated SMCs is decreased compared to uncoated SMCs. SMCs prepared at 25 °C, 40 °C, and 50 °C have a similar loss angle tangent. With the reaction temperature increase to 70 °C, the loss angle tangent begins to increase. Since the loss angle tangent value is also related to the magnetic core loss, the above results are consistent with the core loss results in Figure 7.

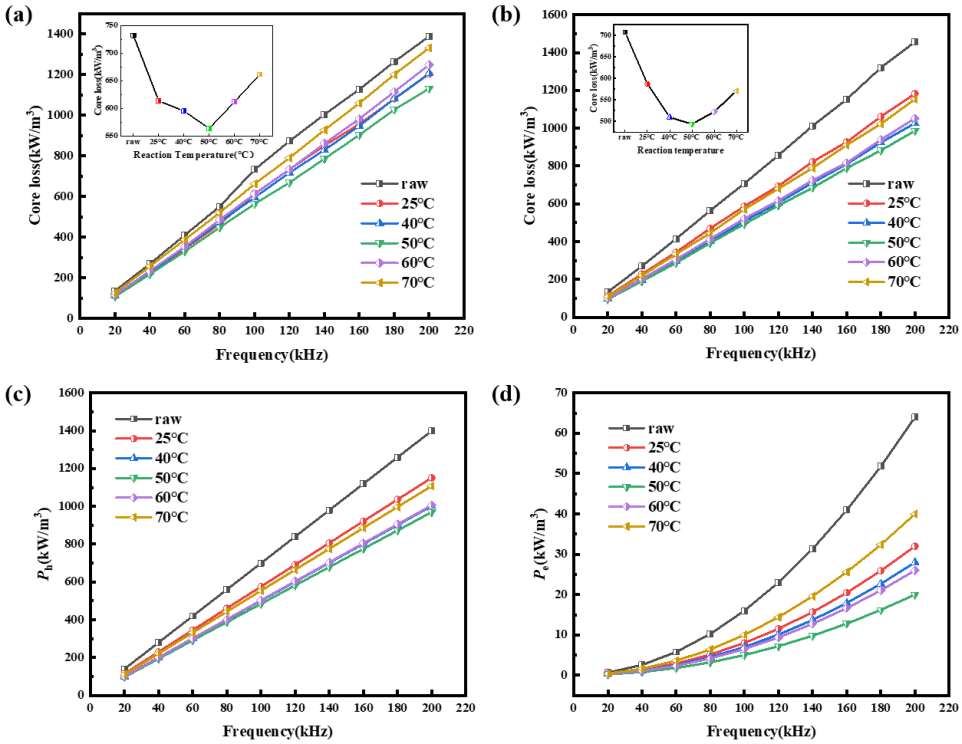

Figure 7. Core loss of SMCs coated by elemental silicon powder through hydrolysis at different reaction temperatures: (**a**) before annealing, (**b**) after annealing, (**c**) P_h after annealing, (**d**) P_e after annealing.

The core loss is the dissipating part of energy that is converted irreversibly into heat through the periodic magnetized process. The total core loss (P_s) is mainly determined by hysteresis loss (P_h), eddy current loss (P_e), and excess loss (P_a), which can be expressed by Equation (6) [30,31]:

$$P_s = P_h + P_e + P_a \approx f \oint H dB + \frac{C_e B^2 d^2 f^2}{\rho} + C_a f^{3/2} \quad (6)$$

where H is the magnetic field, B is the magnetic induction, f is the frequency, C_e and C_a are the constant, d is the thickness of samples, and ρ is resistivity. P_a is a combination of relaxation and resonant loss, which are only important at a low induction and very high frequencies, and can be ignored in power applications [32–34]. It can be separated into P_h and P_e according to Equation (6). The core loss measured in frequency ranging from 20 kHz to 200 kHz under 50 mT external field and separated P_h, P_e are shown in Figure 7, and the inset in Figure 7a,b shows the relationship between the core loss tested under 50 mT/100 kHz and the reaction temperature. In Figure 7c,d, it can be seen that hysteresis loss is the main loss. Compared to the SMCs without SiO_2 coating, the eddy current loss of SMCs coated with SiO_2 is significantly reduced, indicating that the SiO_2 insulation layer can isolate magnetic particles and reduce eddy currents between the magnetic particles. With the introduction of high-resistivity silica coating layer, the resistivity of SMCs increases. The higher reaction temperature results in a higher resistivity of SMCs, indicating the higher content of SiO_2 in the SMCs. With the increase in reaction temperature, the core loss of SMCs before and after annealing first decreases and then increases. The core loss of the

after-annealing SMCs decreased compared to before annealing, except for the raw powder SMCs. The lowest core loss after annealing was 493.3 kW/m^3 at the reaction temperature of 50 °C, with 30% reduction compared to SMCs prepared using the FeSiCr raw powder. This happened because the sample prepared at 50 °C had a complete coating layer. With the reaction temperature further increased to 60 °C and 70 °C, the aggregation of SiO_2 becomes more serious, which leads to the increased coercivity and thus increased core loss. As established, in SMCs, SiO_2 impurities between the particles and stressed regions act as the inning sites that can hinder domain wall motion [35,36], which increases the coercivity and directly increases the hysteresis loss.

Figure 8 shows the magnetic hysteresis curves measured in the range from 18,000 Oe to 18,000 Oe of the external magnetic field and coercivity of the FeSiCr raw powder and FeSiCr@SiO_2 powder prepared with reaction temperatures from 25 °C to 70 °C. The saturation magnetization (M_s) is 169.40 emu/g when the reaction temperature is 50 °C, and the M_s of the FeSiCr raw powder is 173.97 emu/g. The M_s of the FeSiCr magnetic powder decreases monotonously with the increase in reaction temperature. This is because as the reaction temperature increases, more SiO_2 is produced in SMCs. The introduction of non-magnetic SiO_2 results in a magnetic dilution effect, which causes the decreased M_s. Figure 8b shows that the coercivity of the FeSiCr powder decreases first and then increases, consistent with the tendency exhibited by hysteresis loss shown in Figure 7c.

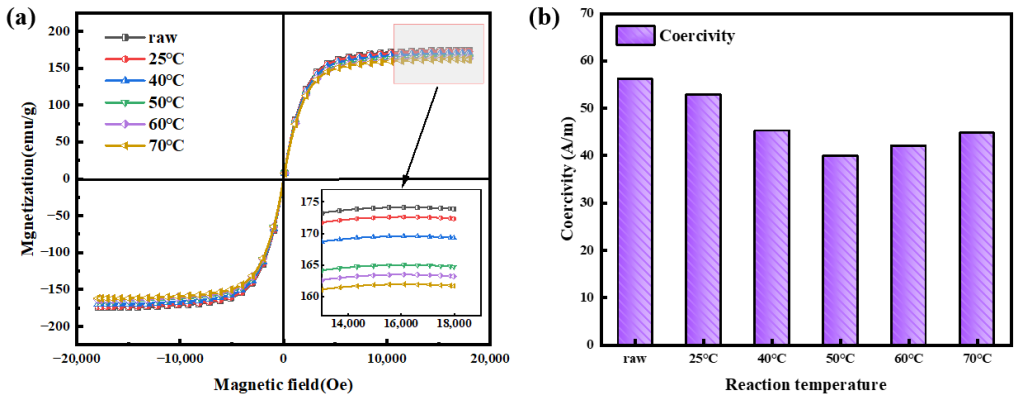

Figure 8. (**a**) Hysteresis curve and (**b**) coercivity of SMCs coated by elemental silicon powder through hydrolysis at different reaction temperatures.

3.3. Effects of Ammonia Concentration on Magnetic Properties

The effects of ammonia concentration on SMCs were further investigated based on the optimized reaction temperature of 50 °C. The amount of ammonia added ranged from 5 mL to 25 mL, which means that the concentration of ammonia ranged from 0.05 mL/g to 0.25 mL/g. Figure 9 and Table 2 show the magnetic properties of SMCs prepared using the elemental silicon hydrolysis method with different ammonia concentrations. Figure 9a shows that the μ_e of FeSiCr SMCs has good frequency stability. With the increase in ammonia concentration, μ_e decreased from 40.55 to 35.50. This is because the increase in ammonia concentration promotes the reaction of the amide group with the hydroxyl group, leading to an increase in the non-magnetic phase and magnetic dilution effect. This can also be understood for the variation of the resistivity in Figure 9d. With the increase in ammonia concentration, the resistivity of the sample increased gradually, indicating the increase in the silica content within the sample.

The Q values of the samples are shown in Figure 9b, and all the samples had the same Q tendency of first increasing then decreasing with the increase in frequency. At 1 MHz, the sample with an ammonia concentration of 0.10 mL/g had the highest quality factor of 57.07. Figure 9c shows the loss angle tangent of the samples coated through hydrolysis, with the ammonia concentrations varying from 0.01 mL/g to 0.25 mL/g in the frequency range from 20 kHz to 5 MHz. With the ammonia concentration increase, the loss angle tangent first decreases and then increases, reaching a minimum at 0.10 mL/g ammonia concentration.

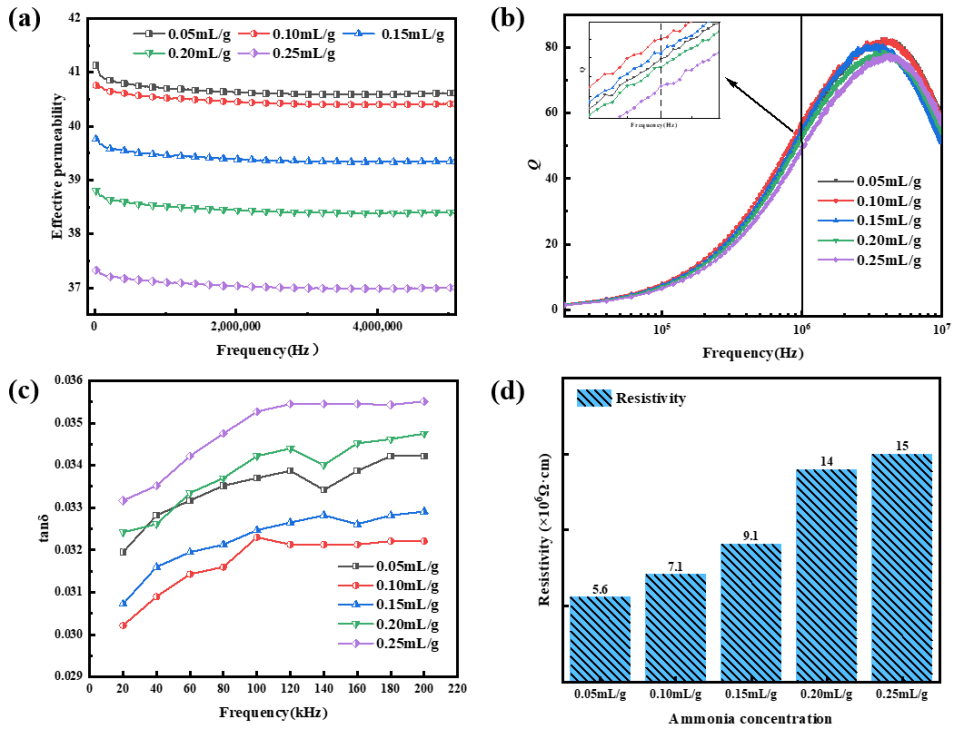

Figure 9. Magnetic properties of SMCs coated with elemental silicon powder through hydrolysis at different ammonia concentrations: (**a**) effective permeability, (**b**) quality factor, (**c**) loss angle tangent, (**d**) resistivity.

Table 2. Magnetic properties of SMCs coated with elemental silicon powder hydrolysis at different ammonia concentrations.

Sample	ρ (Ω·cm)	μ_e (1 MHz)	Q (1 MHz)	P_s (kW/m^3) @ 50 mT	
				100 kHz	200 kHz
0.05 mL/g	5.6×10^6	40.55	53.71	538.8	1091
0.10 mL/g	7.1×10^6	40.46	57.06	493.3	987
0.15 mL/g	9.0×10^6	39.45	54.58	501.2	1013
0.20 mL/g	1.4×10^7	37.10	52.38	546.7	1102
0.25 mL/g	1.5×10^7	35.50	49.57	587.8	1190

The core loss and separated P_h, P_e are shown in Figure 10. In Figure 10c,d, it can be seen that hysteresis loss is the main loss. With the introduction of the silica coating layer, the resistivity of SMCs increases, which results in the reduction in core loss, and the core loss of the after-annealing SMCs decreases compared to before annealing due to the release of internal stresses during the annealing process. On the other hand, the Figure 10a,b inset shows that the core loss at 50 mT/100 kHz first decreases and then increases, reaching a minimum of 493.3 kW/m^3 at 0.10 mL/g ammonia concentration after annealing. The result is also consistent with the tendency of loss angle tangent, shown in Figure 9c. The increase in ammonia concentration can increase the hydrolysis rate and yield of silica, which leads to the decrease in core loss. However, with the further increase in ammonia concentration, the rapid hydrolysis rate results in secondary nucleation, which may influence the size of the silica nanoparticles and the coating effect [25].

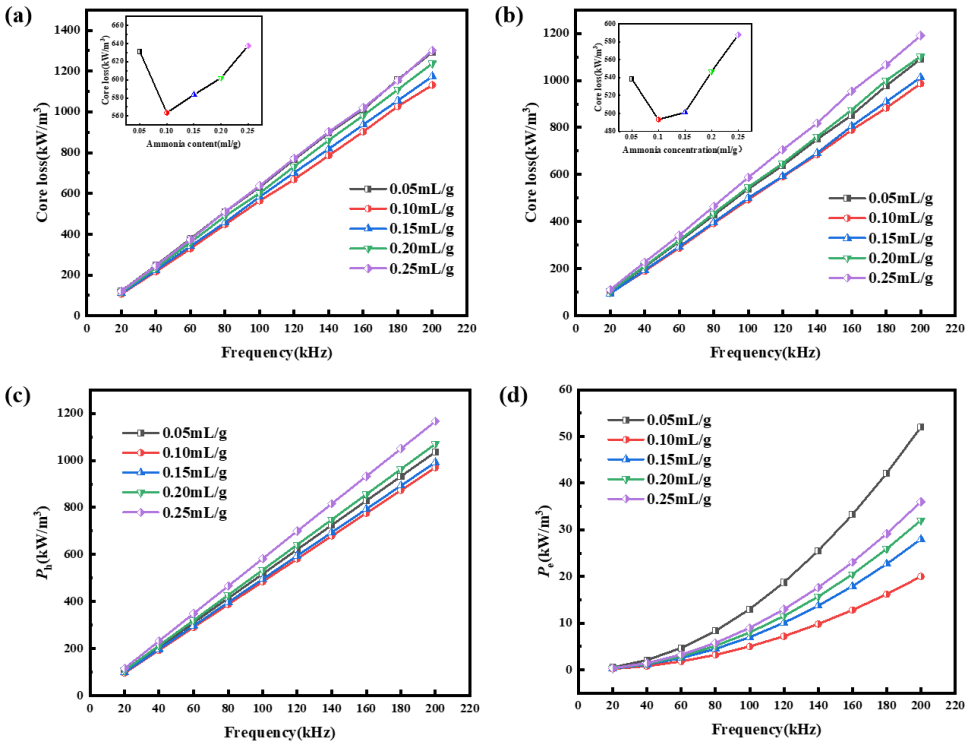

Figure 10. Core loss of SMCs coated by elemental silicon powder hydrolysis at different ammonia concentrations: (**a**) before annealing, (**b**) after annealing, (**c**) P_h after annealing, (**d**) P_e after annealing.

Figure 11 shows the magnetic hysteresis curves and coercivity of the FeSiCr@SiO_2 powder with different ammonia concentrations. The M_s value is 169.40 emu/g when the ammonia concentration is 0.10 mL/g. The M_s of the FeSiCr magnetic powder decreases monotonously with the increase in ammonia concentration due to the magnetic dilution effect. Figure 11b shows that the coercivity of the FeSiCr powder decreases first and then increases, consistent with the tendency exhibited by hysteresis loss shown in Figure 10c.

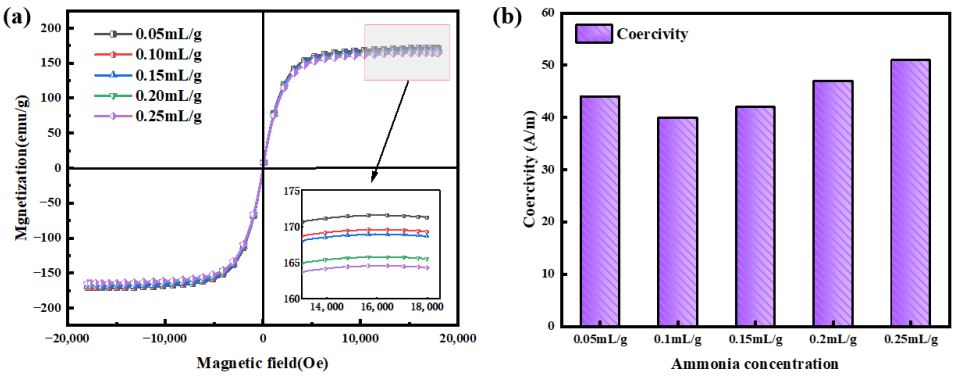

Figure 11. (**a**) Hysteresis curve and (**b**) coercivity of SMCs coated by elemental silicon powder through hydrolysis at different ammonia concentrations.

3.4. Comparison of Magnetic Performance

Based on the above results, for the preparation of FeSiCr@SiO_2 SMCs using the elemental silicon powder hydrolysis method, the optimal reaction temperature and ammonia concentration are 50 °C and 0.10 mL/g, respectively. Through this process, SMCs with an effective permeability of μ_e = 40.46 and magnetic core loss of 493.3 kW/m^3 (50 mT/100 kHz) were obtained. Table 3 compares the magnetic properties of FeSiCr@SiO_2 SMCs obtained in this work and those fabricated using the traditional sol-gel method. The FeSiCr@SiO_2 SMCs fabricated using the sol-gel method were prepared by the author. It is clear that the sample

prepared through the hydrolysis of elemental silicon powder has higher permeability and lower core loss, which indicates that the advantages of our new approach are that it can prepare a thinner and more uniform silica coating layer. However, slightly lower resistivity and quality factor are also obtained in our samples. For conventional sol-gel-prepared SMCs, the high resistivity implies that more SiO_2 is coated on the powder, which leads to the reduction in magnetic permeability. The thicker coating layer can also limit the eddy current loss at a high frequency between the particles, so the quality factor is slightly higher. Compared with the traditional sol-gel method, the coating layer prepared through the hydrolysis of elemental silicon powder is thinner, so its application under high-frequency conditions may be limited, but it has a higher permeability and lower core loss.

Table 3. Permeability, resistivity, and special point core loss and quality factor of SMCs coated using the sol-gel method and elemental silicon powder hydrolysis method.

Sample	ρ (Ω·cm)	μ_e (1 MHz)	Q (1 MHz)	P_s (kW/m^3) @ 50 mT		
				100 kHz	200 kHz	300 kHz
Sol-gel	8.3×10^7	33.96	60.07	648.2	1270	2022
This work	7.1×10^6	40.46	57.07	493.3	987	1650

Figure 12 gives the permeability and core loss of the FeSiCr SMCs fabricated in this work and traditional sol-gel method, and other reported FeSiCr-based SMCs. The FeSiCr SMC prepared through elemental silicon powder hydrolysis coating exhibits a lower magnetic loss and higher μ_e. It is worthy of note that compared with the traditional SiO_2 coating method, this method just needs elemental silicon as the raw material, and no expensive precursor such as TMOS, TEOS, or TPOS is required, so it is more economical [24,25]. In addition, the traditional sol-gel method with either complex processing steps [23,37,38] or long reaction time (up to tens of hours) [39,40] is not conducive to batch production. Hence, this work shows prospect in mass production of high-temperature-resistant silica-coated SMCs with a simplified process and low processing cost, which maybe applied to mass production industries such as mobile phones, automobiles, etc.

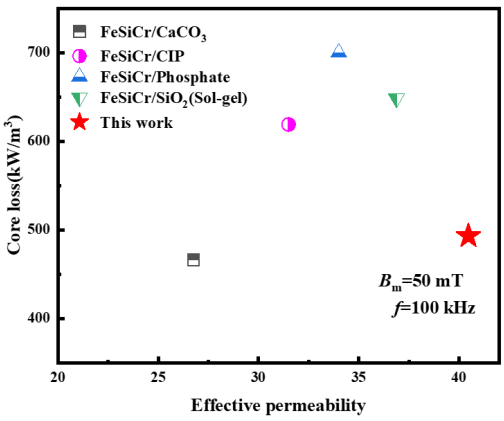

Figure 12. Comparison of the magnetic properties obtained in this work and reported previously for different FeSiCr SMCs, data from [41–43].

4. Conclusions

FeSiCr soft magnetic composites (SMCs) with a SiO_2 insulation layer were prepared through the hydrolysis of elemental silicon powder. The insulation layer effectively optimized the core loss, resistivity and quality factor Q, of the SMCs. The samples prepared with a 0.10 mL/g ammonia concentration at 50 °C exhibited the best combination of magnetic property performance, with saturation magnetization M_s = 169.40 emu/g, effective permeability μ_e = 40.46, resistivity $\rho = 7.1 \times 10^6$ Ω·cm, quality factor Q = 57.07 at 1 MHz, and core loss P_s = 493.3 kW/m^3 at 50 mT/100 kHz. Compared to traditional SiO_2 coating

methods, this approach of coating SiO_2 through elemental silicon powder hydrolysis can reduce the cost and simplify the process, producing a viable solution for the mass production of high-temperature-resistant SMCs.

Author Contributions: Formal analysis, C.L. and H.Y.; Investigation, C.L. and H.Y.; Methodology, C.L., H.Y., G.H. and Z.L.; Project administration, H.Y. and Z.L.; Supervision, H.Y.; Visualization, C.L.; Writing–original draft, C.L.; Writing–review and editing, C.L., H.Y., G.H. and Z.L.; All authors have read and agreed to the published version of the manuscript.

Funding: This work was supported by the Dongguan Innovative Research Team Program (grant no. 2020607231010) and Guangdong Provincial Natural Science Foundation of China (no. 2021A1515010642).

Data Availability Statement: Not applicable.

Conflicts of Interest: The authors declare no conflict of interest.

References

1. Périgo, E.A.; Weidenfeller, B.; Kollár, P.; Füzer, J. Past, present, and future of soft magnetic composites. *Appl. Phys. Rev.* **2018**, *5*, 031301. [CrossRef]
2. Gutfleisch, O.; Willard, M.A.; Brück, E.; Chen, C.H.; Sankar, S.G.; Liu, J.P. Magnetic Materials and Devices for the 21st Century: Stronger, Lighter, and More Energy Efficient. *Adv. Mater.* **2011**, *23*, 821–842. [CrossRef] [PubMed]
3. Li, Q.; Zheng, S.; Mao, Y.; Xu, D.; Peng, Y.; Zhao, Y. Microstructure and properties of amorphous FeSiCrBC soft magnetic composites prepared by using HNO_3 solution. *J. Mater. Sci. Mater. Electron.* **2023**, *34*, 862. [CrossRef]
4. Wu, F.; Liu, Z.; Dong, Y.; Zhang, R.; He, A.; Ling, Y.; Li, J.; Liu, X. Correlation Mechanism of Microstructure, Magnetic Domain, and Magnetic Softness of Fe-6.5 wt.%Si Composites with High Saturation. *J. Supercond. Nov. Magn.* **2023**, *36*, 733–743. [CrossRef]
5. Zhang, C.; Peng, X.; Li, J.; Ellis, T.; Wu, Q.; Xu, J.; Hong, B.; Wang, X.; Ge, H. Design, Preparation, and Magnetic Properties of Fe_4N/Fe_3N Soft Magnetic Composites Fabricated by Gas Nitridation. *J. Supercond. Nov. Magn.* **2023**, *36*, 923–929. [CrossRef]
6. Dosoudil, R.; Franek, J.; Slama, J.; Usakova, M.; Gruskova, A. Electromagnetic Wave Absorption Performances of Metal Alloy/Spinel Ferrite/Polymer Composites. *IEEE Trans. Magn.* **2012**, *48*, 1524–1527. [CrossRef]
7. Wang, X.; Xu, X.; Gong, W.; Feng, Z.; Gong, R. Electromagnetic properties of Fe-Si-Al/$BaTiO_3$/$Nd_2Fe_{14}B$ particulate composites at microwave frequencies. *J. Appl. Phys.* **2014**, *115*, 17C722. [CrossRef]
8. Kim, I.G.; Song, K.H.; Park, B.O.; Choi, B.I.; Choi, H.J. Nano-sized Fe soft-magnetic particle and its magnetorheology. *Colloid Polym. Sci.* **2011**, *289*, 79–83. [CrossRef]
9. Zhu, S.J.; Duan, F.; Feng, S.J.; Liu, X.S.; Kan, X.C.; Lv, Q.R.; Sun, W. Efficient inorganic-coated FeSiAl/WS_2 soft magnetic composites with low magnetic loss. *J. Alloys Compd.* **2023**, *936*, 168190. [CrossRef]
10. Huang, Y.; Zhang, H.; Shang, R.; Wang, K.; Wu, P.; Wang, Y.; Li, F.; Wang, T. Improved magnetic properties in amorphous FeSiBCr soft magnetic composites with easy-plane anisotropy for high-frequency applications. *J. Phys. D Appl. Phys.* **2023**, *56*, 065004. [CrossRef]
11. Huang, H.; Zhang, R.; Sun, H.; Zhang, J.; Wang, J. High density Fe-based soft magnetic composites with nice magnetic properties prepared by warm compaction. *J. Alloys Compd.* **2023**, *947*, 169460. [CrossRef]
12. Garibaldi, M.; Ashcroft, I.; Lemke, J.N.; Simonelli, M.; Hague, R. Effect of annealing on the microstructure and magnetic properties of soft magnetic Fe-Si produced via laser additive manufacturing. *Scr. Mater.* **2018**, *142*, 121–125. [CrossRef]
13. Nie, W.; Yu, T.; Wang, Z.; Wei, X. High-performance core-shell-type FeSiCr@MnZn soft magnetic composites for high-frequency applications. *J. Alloys Compd.* **2021**, *864*, 158215. [CrossRef]
14. Dong, B.; Qin, W.; Su, Y.; Wang, X. Magnetic properties of FeSiCr@MgO soft magnetic composites prepared by magnesium acetate pyrolysis for high-frequency applications. *J. Magn. Magn. Mater.* **2021**, *539*, 168350. [CrossRef]
15. Hsiang, H.-I.; Chuang, K.-H.; Lee, W.-H. FeSiCr Alloy Powder to Carbonyl Iron Powder Mixing Ratio Effects on the Magnetic Properties of the Iron-Based Alloy Powder Cores Prepared Using Screen Printing. *Materials* **2021**, *14*, 1034. [CrossRef]
16. Choi, Y.J.; Ahn, J.H.; Kim, D.H.; Kim, Y.R.; Lee, B.W. Core-loss reduction of Fe–Si–Cr crystalline alloy according to particle size in the high frequency band. *Curr. Appl. Phys.* **2022**, *39*, 324–330. [CrossRef]
17. Ren, X.; Corcolle, R.; Daniel, L. Bounds and estimates on eddy current losses in soft magnetic composites. *J. Appl. Phys.* **2018**, *123*, 235109. [CrossRef]
18. Simizu, S.; Ohodnicki, P.R.; McHenry, M.E. Metal Amorphous Nanocomposite Soft Magnetic Material-Enabled High Power Density, Rare Earth Free Rotational Machines. *IEEE Trans. Magn.* **2018**, *54*, 1–5. [CrossRef]
19. Kim, H.J.; Nam, S.M.; Koh, J.H. Fe-Si-Cr/PTFE magnetic composite thick films on polyethylene terephthalate sheets for near field communications by aerosol deposition. *J. Nanosci. Nanotechnol.* **2014**, *14*, 7915–7918. [CrossRef] [PubMed]
20. Hsiang, H.-I.; Wang, S.-K.; Chen, C.-C. Electromagnetic properties of FeSiCr alloy powders modified with amorphous SiO_2. *J. Magn. Magn. Mater.* **2020**, *514*, 167151. [CrossRef]

21. Wu, S.; Sun, A.; Lu, Z.; Cheng, C.; Gao, X. Magnetic properties of iron-based soft magnetic composites with SiO_2 coating obtained by reverse microemulsion method. *J. Magn. Magn. Mater.* **2015**, *381*, 451–456. [CrossRef]
22. Luo, Z.; Fan, X.A.; Hu, W.; Luo, F.; Li, G.; Li, Y.; Liu, X.; Wang, J. Controllable SiO_2 insulating layer and magnetic properties for intergranular insulating Fe-6.5 wt.%Si/SiO_2 composites. *Adv. Powder Technol.* **2019**, *30*, 538–543. [CrossRef]
23. Cheng, J.; Ni, X.; Zheng, H.; Li, B.; Zhang, X.; Zhang, D. Preparation of Fe (core)/SiO_2 (shell) composite particles with improved oxidation-resistance. *Mater. Res. Bull.* **2006**, *41*, 1424–1429. [CrossRef]
24. Lim, H.M.; Lee, J.; Jeong, J.-H.; Oh, S.-G.; Lee, S.-H. Comparative Study of Various Preparation Methods of Colloidal Silica. *Engineering* **2010**, *2*, 998–1005. [CrossRef]
25. Guo, J.; Liu, X.; Cheng, Y.; Li, Y.; Xu, G.; Cui, P. Size-controllable synthesis of monodispersed colloidal silica nanoparticles via hydrolysis of elemental silicon. *J. Colloid Interface Sci.* **2008**, *326*, 138–142. [CrossRef]
26. Lim, H.M.; Shin, H.C.; Huh, S.H.; Lee, S.H. Effect of Catalyst on the Colloidal Silica Particle Growth in Direct Oxidation of Silicon. *Solid State Phenom.* **2007**, *124–126*, 667–670. [CrossRef]
27. Wang, S.; Tang, J.; Zhao, H.; Wan, J.; Chen, K. Synthesis of magnetite–silica core–shell nanoparticles via direct silicon oxidation. *J. Colloid Interface Sci.* **2014**, *432*, 43–46. [CrossRef]
28. Wu, C.; Huang, M.; Luo, D.; Jiang, Y.; Yan, M. SiO_2 nanoparticles enhanced silicone resin as the matrix for Fe soft magnetic composites with improved magnetic, mechanical and thermal properties. *J. Alloys Compd.* **2018**, *741*, 35–43. [CrossRef]
29. Wang, C.; Guo, Z.; Wang, J.; Sun, H.; Chen, D.; Chen, W.; Liu, X. Industry-oriented Fe-based amorphous soft magnetic composites with SiO_2-coated layer by one-pot high-efficient synthesis method. *J. Magn. Magn. Mater.* **2020**, *509*, 166924. [CrossRef]
30. Olekšáková, D.; Kollár, P.; Jakubčin, M.; Füzer, J.; Tkáč, M.; Slovenský, P.; Bureš, R.; Fáberová, M. Energy loss separation in NiFeMo compacts with smoothed powders according to Landgraf's and Bertotti's theories. *J. Mater. Sci.* **2021**, *56*, 12835–12844. [CrossRef]
31. Olekšáková, D.; Kollár, P.; Neslušan, M.; Jakubčin, M.; Füzer, J.; Bureš, R.; Fáberová, M. Impact of the Surface Irregularities of NiFeMo Compacted Powder Particles on Irreversible Magnetization Processes. *Materials* **2022**, *15*, 8937. [CrossRef]
32. Shokrollahi, H.; Janghorban, K. Soft magnetic composite materials (SMCs). *J. Mater. Process. Technol.* **2007**, *189*, 1–12. [CrossRef]
33. Wu, Z.Y.; Jiang, Z.; Fan, X.A.; Zhou, L.J.; Wang, W.L.; Xu, K. Facile synthesis of Fe-6.5 wt%Si/SiO_2 soft magnetic composites as an efficient soft magnetic composite material at medium and high frequencies. *J. Alloys Compd.* **2018**, *742*, 90–98. [CrossRef]
34. Chang, C.; Guo, J.; Li, Q.; Zhou, S.; Liu, M.; Dong, Y. Improvement of soft magnetic properties of FeSiBPNb amorphous powder cores by addition of FeSi powder. *J. Alloys Compd.* **2019**, *788*, 1177–1181. [CrossRef]
35. Talaat, A.; Suraj, M.V.; Byerly, K.; Wang, A.; Wang, Y.; Lee, J.K.; Ohodnicki, P.R. Review on soft magnetic metal and inorganic oxide nanocomposites for power applications. *J. Alloys Compd.* **2021**, *870*, 159500. [CrossRef]
36. Kollár, P.; Birčáková, Z.; Füzer, J.; Bureš, R.; Fáberová, M. Power loss separation in Fe-based composite materials. *J. Magn. Magn. Mater.* **2013**, *327*, 146–150.
37. Ammar, M.; Mazaleyrat, F.; Bonnet, J.P.; Audebert, P.; Brosseau, A.; Wang, G.; Champion, Y. Synthesis and characterization of core–shell structure silica-coated $Fe_{29.5}Ni_{70.5}$ nanoparticles. *Nanotechnology* **2007**, *18*, 285606. [CrossRef]
38. Wang, J.; Fan, X.A.; Wu, Z.; Li, G. Regulation and control of insulated layers for intergranular insulated Fe/SiO_2 soft magnetic composites. *J. Mater. Sci.* **2017**, *52*, 7091–7099. [CrossRef]
39. Lu, X.; Liang, G.; Sun, Q.; Yang, C. High-frequency magnetic properties of $FeNi_3$–SiO_2 nanocomposite synthesized by a facile chemical method. *J. Alloys Compd.* **2011**, *509*, 5079–5083. [CrossRef]
40. Fan, X.A.; Wang, J.; Wu, Z.; Li, G. Core–shell structured FeSiAl/SiO_2 particles and Fe_3Si/Al_2O_3 soft magnetic composite cores with tunable insulating layer thicknesses. *Mater. Sci. Eng. B* **2015**, *201*, 79–86. [CrossRef]
41. Wang, F.; Dong, Y.; Chang, L.; Pan, Y.; Chi, Q.; Gong, M.; Li, J.; He, A.; Wang, X. High performance of Fe-based soft magnetic composites coated with novel nano-$CaCO_3$/epoxy nanocomposites insulating layer. *J. Solid State Chem.* **2021**, *304*, 122634. [CrossRef]
42. Gong, M.; Dong, Y.; Huang, J.; Chang, L.; Pan, Y.; Wang, F.; He, A.; Li, J.; Liu, X.; Wang, X. The enhanced magnetic properties of FeSiCr powder cores composited with carbonyl iron powder. *J. Mater. Sci. Mater. Electron.* **2021**, *32*, 8829–8836. [CrossRef]
43. Yu, H.; Zhou, S.; Zhang, G.; Dong, B.; Meng, L.; Li, Z.; Dong, Y.; Cao, X. The phosphating effect on the properties of FeSiCr alloy powder. *J. Magn. Magn. Mater.* **2022**, *552*, 168741. [CrossRef]